Neural-Augmented Space Weather Forecasting for Uncertainty Propagation in LEO Conjunction Analysis

Saikat Majumder
Digantara Research and Technologies Pvt. Ltd., India
Archana Trivedi
Digantara Research and Technologies Pvt. Ltd., India
Bhanu Chandana
Digantara Research and Technologies Pvt. Ltd., India
Subramanian Arumugam
Digantara Research and Technologies Pvt. Ltd., India
Thamim Ansari
Digantara Research and Technologies Pvt. Ltd., India
Tanveer Ahmed
Digantara Research and Technologies Pvt. Ltd., India

ABSTRACT

Accurate orbit prediction and collision risk assessment for low-Earth orbit (LEO) satellites are highly dependent on precise thermospheric density modeling, which is strongly influenced by space weather drivers such as solar radio flux (F10.7) and the planetary geomagnetic index (Kp). In this work, we develop and evaluate machine learning (ML) forecasts of these drivers using CelesTrak and OMNI datasets, employing a multivariate Variational Mode Decomposition (VMD) and Long Short-Term Memory (LSTM) architecture, referred to as the VL model, to effectively capture nonlinear and dynamic space weather variations. These forecasts are ingested into the NRLMSISE-00 density model within Digantara's proprietary high fidelity orbit propagator (EPIC) to drive orbit prediction for synthetic LEO satellites spanning low to high altitudes and having configurations from 1U to 16U. In the simulation framework, only the atmospheric density input is varied, while all other force and drag parameters are held constant. Forecast-driven orbits are compared against truth-driven references under space weather conditions ranging from quiet to extreme, quantifying prediction sensitivities with altitude and object size. By propagating forecasted states and uncertainties, we further map model-driven density errors into collision probability (Pc) estimation during representative conjunction scenarios.

Our results show that objects propagated using VL model outputs demonstrate improved predictive accuracy as compared to current operational space weather driver forecasts. For a historical conjunction event, VL models closely reproduce Pc values computed using observed space weather parameters at shorter lead times, thereby improving the timeliness and reliability of conjunction assessments. These results highlight the operational value of integrating ML-driven space weather forecasting with operational neutral density modeling to enhance orbit determination and improve conjunction analysis capabilities.

Copyright © 2025 Advanced Maui Optical and Space Surveillance Technologies Conference (AMOS) – www.amostech.com

1. INTRODUCTION

The proliferation of satellites in low-Earth orbit (LEO) has created an increasingly congested space environment, necessitating sophisticated conjunction assessment and collision avoidance capabilities for satellite operations. Accurate orbit prediction and collision risk assessment for LEO satellites are fundamentally dependent on precise modeling of thermospheric neutral mass density, which is highly influenced by space weather drivers such as the solar radio flux (F10.7) and the planetary geomagnetic index (Kp). The variability in neutral mass density represents one of the most dominant sources of uncertainty in LEO satellite trajectory prediction. Errors in the characterization or forecast of drivers such as F10.7 and Kp translate directly into orbit-prediction errors and into uncertainties in collision-probability (Pc) calculations [1].

Current operational space weather forecasts typically rely on climatological persistence models that introduce significant uncertainties during dynamic space weather events. These methods are simple and robust under quiet conditions, but they frequently fail to capture nonlinear, nonstationary behavior during transient or extreme geomagnetic activity, producing forecasts with poorly characterized and sometimes large uncertainties. These forecasting uncertainties can result in position errors exceeding several kilometers for 1-day propagations during major geomagnetic storms, creating substantial challenges for reliable collision risk assessment and maneuver decision-making [2]. The critical importance of uncertainty quantification in space weather forecasting has become increasingly apparent as satellite operators must make collision avoidance decisions 12-24 hours in advance, often without adequate confidence measures regarding the reliability of forecast models.

Reference [1] developed climatological forecast models for F10.7 and Kp that accurately capture the heteroscedastic and highly non-Gaussian uncertainty distributions inherent in space weather driver forecasts. Their methodology demonstrated that improved driver forecasts, particularly for F10.7, enable durable maneuver decisions with additional lead time of up to 24 hours during examined periods. The study utilized realistic satellite conjunction scenarios to quantify how space weather driver forecast uncertainty contributes to collision probability estimation and maneuver decisions, revealing that forecast improvements are most beneficial above 500 km altitude.

Another work [3] incorporated uncertainties in projected F10.7 and Ap indices into per-object covariances at time of closest approach (TCA), demonstrating that accounting for these uncertainties can lead to significantly different estimates of collision probability. Their approach utilized probability distribution functions of historical forecast errors for F10.7 and Ap as functions of prediction horizon, generating ensemble density scenarios through NRLMSISE modeling. The methodology involved propagating different ensembles consisting of thousands of members through various thermospheric conditions to assess collision risk under varying solar activity.

Reference [4] advanced the field by quantifying and propagating model uncertainty while including correlation factors between position uncertainties of conjuncting objects, recognizing that both objects often travel through similar perturbed atmospheric regions. The conjunction assessment community has increasingly emphasized covariance-realism efforts to ensure maneuver decisions are based on accurate projected uncertainties, with many operators now including atmospheric density errors in covariance calculations through consider parameters and process noise tuning.

1.1 Machine Learning Approaches for Space Weather Forecasting

1.1.1 F10.7 Forecasting Models

Recent advances in data-driven methods present promising alternatives for space-weather forecasting. Recurrent neural networks such as Long Short-Term Memory (LSTM) models [5] have been shown to improve prediction of geomagnetic indices like Kp by capturing temporal dependencies better than simpler regression methods [4]. Hybrid techniques that combine signal decomposition with sequence models, for example Variational Mode Decomposition (VMD) followed by LSTM, have produced improvements in F10.7 forecasting by isolating intrinsic modes prior to sequence modeling [5]. Multivariate machine learning (ML) models that predict multiple driver indices simultaneously further enable a more comprehensive treatment of driver correlations for downstream use.

The application of machine learning (ML) techniques to F10.7 forecasting has evolved significantly, with several innovative approaches demonstrating superior performance compared to traditional methods. Temporal convolutional networks (TCN) for F10.7 prediction was used by [6], achieving high correlation coefficients ($R = 0.98$) and low root mean square errors (RMSE = 5.04 – 5.18 sfu) for 1-3 day forecasts. The TCN model combines aspects of recurrent neural networks and convolutional neural networks, utilizing causal and extended convolutional structures that avoid gradient problems inherent in traditional RNN architectures while enabling efficient parallel computation.

Copyright © 2025 Advanced Maui Optical and Space Surveillance Technologies Conference (AMOS) – www.amostech.com

Variational Mode Decomposition (VMD) combined with LSTM networks [7] has emerged as a particularly effective hybrid approach for F10.7 forecasting. This methodology decomposes the original F10.7 time series into several intrinsic mode functions (IMFs) with different frequency characteristics using VMD, then applies LSTM neural networks to forecast each component separately before reconstructing the final prediction. The VMD-LSTM approach has demonstrated superior accuracy compared to individual LSTM models and traditional methods, particularly effective for 1 to 27-day forecasting horizons.

Transformer-based architectures, particularly the Informer model, have shown remarkable success in medium-term F10.7 forecasting [8]. This model uses 48 historical daily F10.7 indices as input to forecast 1-27 days ahead, demonstrating superior performance compared to statistical methods from British Geological Survey (BGS) and NOAA Space Weather Prediction Center (SWPC), especially during the descending phase of the solar cycle.

1.1.2 Kp Forecasting Models

The development of machine learning models for Kp index forecasting has explored various architectures and methodologies, each demonstrating distinct advantages in capturing the complex nonlinear relationships between solar wind parameters and geomagnetic activity.

Reference [9] implemented a multilayer perceptron (MLP) model using a recurrent neural network architecture with a guided closed-loop approach for extended prediction horizons. The model architecture consisted of an input layer, a single nonlinear hidden layer with 28 neurons, and a linear output layer that predicts Kp up to 24 hours in advance. The training utilized three decades (1986-2016) of historical data from NASA's OMNI database, with testing conducted on 2017 data. The model incorporated six solar wind and interplanetary magnetic field (IMF) parameters: Bz (north-south component of IMF), proton number density (n), plasma speed (V), IMF magnitude (|B|), RMS standard deviation of the IMF (σB), and historical Kp values with time lags up to τ = 24-30 hours. Performance evaluation demonstrated correlation coefficients ranging from 0.7510 to 0.8211 with RMSE values between 0.8949 and 0.9302 for 24-hour predictions across 272 forecast days.

Reference [5] performed a comprehensive analysis comparing the effectiveness of solar wind-based predictions, recurrence-based predictions, and persistence models using artificial neural networks. Their methodology explored forecast horizons from short-term (approximately half a day) to long-term (more than 2 days), demonstrating that predictions based on historical Kp recurrence patterns provided comparable or superior accuracy to solar wind measurements alone. The study revealed that solar wind measurements at L1 provide minimal improvement for forecasts with long horizon times, while the addition of historical Kp values to solar wind measurements offers barely noticeable improvement for short-term forecasts.

LSTM-based forecasting models for geomagnetic index prediction are developed in [10], using both solar wind parameters and historical Kp values as inputs. The LSTM architecture was selected for its superior capability in handling sequential time series data and capturing long-term dependencies inherent in space weather systems. The model demonstrated improved Kp forecasting performance compared to traditional methods, achieving lower mean absolute error and mean squared error metrics. The LSTM approach utilized solar wind and interplanetary magnetic field parameters as primary inputs while incorporating the temporal evolution of the Kp index itself to enhance prediction accuracy.

Another study [11] proposed a classification-based approach that utilizes predicted data from individual geomagnetic observatories. By treating each observatory independently within the forecasting process, the method enables index predictions that remain consistent with the physical principles underlying the original Kp index computation. The model demonstrates performance for both Kp and the newer Hpo indices (Hp60 and Hp30), which measure planetary disturbances with higher temporal resolution (hourly and half-hourly respectively) than the traditional 3-hourly Kp index and without the upper limit constraint of 9. The approach utilizes solar wind parameters from high-resolution NASA OMNI dataset including IMF Bt, proton density, solar wind speed, and Sunspot number, providing 3-day nowcast and 3-day forecast capabilities. The model shows good agreement in capturing trends and overall behavior even with sparse solar wind data, representing a significant advancement in observatory-based geomagnetic forecasting.

Building on this line of research, the existing literature clearly demonstrates a shift toward multivariate forecasting frameworks that aim to predict several space weather indices simultaneously. This allows for more comprehensive and physically consistent modeling of the coupled solar-terrestrial system. Despite this progress, most studies to date have been constrained to short prediction horizons, typically up to 24-hours where model performance remains robust. However, forecast skill deteriorates rapidly at longer lead times, leaving a critical gap in operational space weather

Copyright © 2025 Advanced Maui Optical and Space Surveillance Technologies Conference (AMOS) – www.amostech.com

prediction, especially for applications such as satellite drag estimation and conjunction assessment where multi-day forecasts are essential.

To address this gap, the present work develops an ML-based VMD-LSTM forecasting algorithm designed to extend prediction capabilities up to 3 days. Specifically, we employ a 27-day input history for F10.7 forecasting, capturing the solar rotational modulation of extreme ultraviolet flux, and a 3-day input history for Kp forecasting, leveraging short-term magnetospheric response patterns to solar wind drivers. The outputs from these ML models are then coupled with a high-fidelity orbit propagator to evaluate the downstream effects of forecast uncertainties. This integrated framework allows us to systematically examine how errors in ML-based F10.7 and Kp forecasts propagate into thermospheric density modeling, orbit prediction, and probabilistic conjunction assessment for synthetic LEO objects spanning a range of altitudes and form factors.

The rest of the paper is outlined as follows: Section **2** describes the ML model development, orbit propagation framework and collision probability estimation methodology. In Section **3**, we present the model performance results and assess their performance against established benchmarks. Section **4** summarizes the key findings of the paper and provides directions for future research.

2. METHODOLOGY

2.1 ML Model Development

This study employs a unified, hybrid forecasting framework based on Variational Mode Decomposition (VMD) and Long Short-Term Memory (LSTM) networks [7]. The overarching philosophy is to decompose complex, dynamic heliophysical and geophysical time series into simpler sub-components and model each component separately to obtain enhanced predictive accuracy. While the core algorithm remains consistent, specific implementations are tailored to the unique characteristics of the F10.7 solar radio flux and the Kp geomagnetic index. The following sections detail the common framework, the explicit differences in its application, and the resulting performance metrics.

2.1.1 The Hybrid VMD-LSTM Framework for Solar and Geomagnetic Forecasting

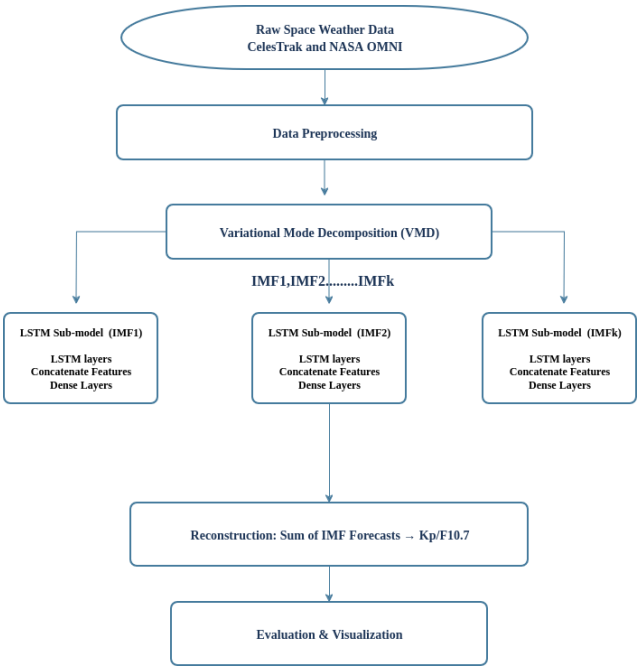

Figure 1: A schematic of the hybrid VMD-LSTM architecture used in this work

The system architecture diagram of the hybrid VMD-LSTM method, hereafter referred to as the **VL Model**, is shown in **Figure 1**.

Copyright © 2025 Advanced Maui Optical and Space Surveillance Technologies Conference (AMOS) – www.amostech.com

The following model development elements are utilized in both the F10.7 and Kp VL forecasting methodologies:

Core Architecture: Both models adopt a decompose-forecast-reconstruct paradigm. The target time series is first decomposed into its intrinsic mode functions (IMFs) using VMD method. This is followed by forecast generation for these IMFs.

Decomposition Technique: Both models use Variational Mode Decomposition (VMD) [12] for the signal analysis. VMD is preferred for its non-recursive, robust nature and ability to isolate band-limited modes with specific sparsity properties.

Base Predictor: Both models use Long Short-Term Memory (LSTM) networks [13] as the core forecasting engine for the decomposed components. LSTMs are chosen for their demonstrated ability to capture long-term dependencies and temporal patterns in time-series data.

Data Source: Space weather data for training and testing were obtained from CelesTrak[1] Space Data and NASA GSFC's OMNIWeb[2] portal. For model training, over 5 decades of F10.7 data is used, while for Kp, about 20 years of Kp and other solar wind parameters are taken.

Data Preprocessing: Both models involve:

- Cleaning: Handling missing values and outliers.
- Temporal Alignment: Ensuring data is on a consistent time grid.
- Train-Validation-Test Split: Using a temporal hold-out method to prevent look-ahead bias and ensure realistic performance evaluation.

Forecast Reconstruction: The final forecast for both F10.7 and Kp is generated by summing the predictions of all individual VMD modes and applying an inverse transformation to the original scale.

Evaluation Metrics: Model performance for both targets are rigorously assessed using a standard suite of metrics including Root Mean Squared Error (RMSE) and Mean Absolute Error (MAE).

Input Data and Feature Engineering

While the framework is shared, critical differences exist in the model design, reflecting the distinct nature of the two physical phenomena. These differences are summarized in **Table 1** and detailed thereafter.

Table 1: Key differences between the F10.7 and Kp forecasting models

Aspect	**F10.7 cm Flux Forecast**	**Kp Index Forecast**
Model Type	Univariate	Multivariate
Primary Input	Past values of F10.7 only	Past values of Kp and solar wind parameters
Feature Engineering	Minimal (only Day-of-Year)	Extensive – Creates physics-based features like cross-terms, (vBs) pressure, derivatives
Predictor Variables	X = [VMD Modes(t-1:t-l), Day-of-Year]	X = [VMD Mode K(t-1:t-l), Avg(Solar_Wind_Features)]
LSTM Design	Single model forecasts all modes	Multiple specialized models (one per mode)
Physical Driver	Solar magnetic activity	Solar wind-magnetosphere coupling

VL F10.7 Model

This is a univariate model. The primary input is the historical F10.7 time series. The other feature is a normalized day of year (doy) value to capture weak annual periodicity. The model relies on the VMD-LSTM structure to intrinsically learn the solar rotation (27-day) and solar cycle (11-year) patterns from the data itself to produce forecasts.

A single LSTM model is constructed for F10.7. The input is a window containing the recent history of all VMD modes plus the temporal feature. The output is a simultaneous prediction of the future values for all VMD modes. This design assumes the modes are interdependent and best learned together.

[1] https://celestrak.org/SpaceData/

[2] https://omniweb.gsfc.nasa.gov/

Copyright © 2025 Advanced Maui Optical and Space Surveillance Technologies Conference (AMOS) – www.amostech.com

The model follows a data-centric approach. The complexity is managed internally through decomposition, trusting the LSTM to learn the underlying temporal dynamics without external physical drivers.

VL Kp Model

This is a multivariate, physics-informed model. Recognizing that Kp occurs in response to various external drivers, the model incorporates crucial exogenous variables:

- ***Physical Parameters:*** Interplanetary Magnetic Field (IMF) components (Bz, By), solar wind speed (V_{SW}), and proton density (N_P).
- ***Coupling Parameters:*** Physically motivated parameters were derived, including:
  - vBs: The product of V_{SW} and the southward IMF component (Bz), a proxy for the dayside reconnection rate.
  - Dynamic Pressure: This parameter governing magnetospheric compression is calculated as:

$$P_{dyn} = 1.6726 \times 10^{-6} \times N_P \times V_{SW}^2$$

- ***Temporal Derivatives:*** The rate-of-change (d/dt) of Bz and V_{SW} to capture sudden changes.

K separate LSTM models are trained for Kp, where K is the number of VMD modes. Each model performs as an expert on a single, specific mode. The models have a dual-input structure:

- Input 1: The recent history of its assigned VMD mode.
- Input 2: A context vector is created representing the average state of the solar wind features over the lookback window. This design allows each model to learn how a specific component (e.g., background, perturbation) of the Kp response is uniquely influenced by the solar wind drivers.

The Kp forecasting model explicitly incorporates the known causal relationship between the solar wind/IMF parameters and geomagnetic activity. The hybrid model acts as a non-linear function approximator for this complex physical relationship.

2.2 Space Weather Forecasting Models

Leveraging a hybrid framework based on the VMD-LSTM forecasting models, we have used a suite of ML-based space weather forecasting models in this study:

- **VL F10.7:** This model is developed by training with more than 5 decades of historical F10.7 data. It generates 3 days forecasts by taking the past 27 days of F10.7 history from the input date. The space weather file used by NRLMSISE-00 model is modified only with the F10.7 forecasts while retaining observed Kp values.
- **VL Kp:** Trained using historical Kp data, solar wind IMF parameters and coupled terms for over 2 decades. This model generates 3 days forecast by taking 3 days of previous Kp values and input features before the input date. The corresponding space weather file is modified only with the Kp forecasts (and subsequently, ap values), keeping the F10.7 values same as the truth.
- **VL F10.7-Kp:** This model is simply a combination of the above two F10.7 and Kp models. Here, another space weather file is generated with Kp, ap and F10.7 files updated with the VL model predictions.

To evaluate the forecast accuracy of these VL models, we will compare the outputs against the open-source space weather forecasts made available at CelesTrak. Another space weather file is generated for the CelesTrak case, hereby abbreviated to CT:

- **CT F10.7-Kp:** The space weather file used for the comparative analysis contains 3-day forecasts of both Kp/ap and F10.7.

All of the above forecasting models for F10.7 and/or Kp are subsequently used in the orbit propagation framework, where their impact on accurate trajectory prediction and collision probability (Pc) estimation is tested as described in the following sections.

2.3 Orbit Propagation Analysis

To assess the performance of the VL space weather models as compared to current space weather forecasts offered by CT, we have designed a robust testing framework using Digantara's high-fidelity orbit propagator, *EPIC*.

Copyright © 2025 Advanced Maui Optical and Space Surveillance Technologies Conference (AMOS) – www.amostech.com

2.3.1 Synthetic Satellite Configurations

Orbit propagation is carried out for four synthetic CubeSats with 1U, 6U, 12U and 16U form factors at different altitudes within LEO. **Table 2** lists the object characteristics and orbital parameters for the synthetic satellites used in this work.

Table 2: Satellite characteristics and orbital parameters for the synthetic satellites

Satellite	Altitude (km)	Inclination (°)	Mass (kg)	Max Cross-sectional Area (m^2)
1 U	(450, 850)	(97.214, 98.816)	8	0.05195
6 U			16	0.343471
12 U			32	0.387991
16 U			36	0.502839

2.3.2 Orbit Propagator Specification

EPIC is a high-fidelity numerical orbit propagator which uses advanced mathematical and astrodynamics algorithms to accurately predict spacecraft trajectories, accounting for various orbital perturbations like gravity, drag, solar radiation, relativistic effects, Earth albedo, and maneuvers. Its optimized processing enables fast computations for large datasets. This combination of sophisticated techniques and computational efficiency aided in conducting the propagation analysis smoothly.

For this analysis, both atmospheric drag and gravitational perturbations were enabled in the propagation framework. The case study incorporates the VL and CT space weather model forecasts into the NRLMSISE-00 density model within *EPIC* to assess how space weather forecast uncertainties influence orbital trajectory predictions for the synthetic satellites. Simulated satellite orbits were first generated using historical space weather observations as ground truth. These orbits are used as reference true orbits for comparison against orbits generated using both CT and VL forecast data. Orbit propagation is performed for a span of 3 days by changing only the underlying space weather data within the NRLMSISE-00 density model while keeping all other propagation parameters constant for respective objects. **Table 3** outlines all force models used for propagation in this analysis.

Table 3: *EPIC* orbit propagator configuration for the analysis

FEATURES	MODEL/CONVENTION/METHODS
Gravity Potential	GGM03S – 70 × 70 (degree and order)
Atmospheric Drag	NRLMSISE-00 (Varying Space Weather), $C_D = 2.2$
Numerical Integrators	DOP853

2.3.3 Space Weather Events

The synthetic satellites are propagated for two events – one during a period with low geomagnetic activity or quiet-time (G0) and another during a period with high geomagnetic activity or storm-time (G4) case. The events are selected to assess the performance of the VL models during low to high space weather activity. To compare the VL model results against CT forecasts, we selected two recent events in 2025. **Table 4** below details the list of two space weather events along with their corresponding space weather parameters during which the synthetic satellite orbits are predicted.

Table 4: Time periods of orbit propagation test cases and their corresponding space weather conditions

Time Period	Kp Range	F10.7 Range (sfu)	NOAA G-Scale	Event Type
2025-07-01 – 2025-07-03	1- to 4-	129.3 to 134.1	G0	Quiet
2025-05-31 – 2025-06-02	2- to 8-	139.9 to 164.2	G4	Severe

Copyright © 2025 Advanced Maui Optical and Space Surveillance Technologies Conference (AMOS) – www.amostech.com

2.4 Collision Probability Estimation

To assess the practical implications of our space weather forecasting and orbit prediction approach, we turn to collision probability (Pc) estimation. This provides a direct way to evaluate how different space weather forecast models influence predicted conjunction risks. In conjunction risk assessments, Pc of two objects under conjunction at the time of closest approach (TCA) is calculated using their predicted state vectors, state covariances and their presumed hard body radii. In this work, we use the numerical Pc calculation algorithm of Foster [14] to compute Pc of two reference objects.

The VL model forecasts developed in this work are used in an example satellite conjunction scenario taken from CelesTrak's SOCRATES database [15], which provides a list of all possible conjunctions occurring in a week. The conjunction scenario of interest is selected during the onset of the May 2024 Gannon storm (G5 level), which is notable for causing huge density enhancements and sudden orbital perturbations in LEO satellite trajectories [2]. The physical characteristics and orbital parameters of the objects of interest are listed in **Table 5** below. The distance of closest approach (DCA) of these objects at TCA is 0.274 km.

Table 5: Object characteristics and orbital parameters for the objects considered.

Satellite	NORAD-ID	Altitude (km)	Inclination (°)	Mass (kg)	Max Area (m^2)	Span (m)
STARLINK-30072	57501	565	43	730	33.884	29
CSC-2	58021	525	97.6	10	0.098	0.5

For both objects, initial states 1 day prior to TCA were obtained using Two Line Element Sets (TLEs) fetched from Space-Track[3]. Using these set of initial states, both the primary and secondary objects are first propagated for a 1-day duration till TCA using true space weather data considering only gravity perturbation with Earth's J2 oblateness (GGM03S – 2 × 0) and atmospheric density. Alongside ephemeris, covariance matrices are also generated considering uncertainties due to gravity and drag perturbations. The initial covariance matrix is assumed to represent a standard level of uncertainty in the initial state estimates, reflecting typical sensor and model inaccuracies at the start of propagation. The states and covariances obtained using this method are treated as the reference trajectory, comprising of both ephemeris and covariance respectively. The objects are then propagated at every 3-hour intervals till TCA using the initial states and covariances from the reference ephemeris and covariances at that timestamp. At the end of each run, the probability of collision is estimated using the final state and covariance. This process is repeated for all three VL models (VL F10.7, VL Kp, VL F10.7-Kp) to examine the impact of space weather forecast in Pc evaluation. We follow this method of calculating iterative collision probability from [1] as it allows us to compare how Pc evolves with time during variable space weather uncertainties.

3. RESULTS AND DISCUSSION

3.1 ML Model Performance During Quiet and Storm Periods

3.1.1 Results and Validation

Validations were performed for both VL F10.7 and Kp models. The results show good forecast performance for training, testing and validation data sets. **Figure 2** below shows the actual versus predicted values of the F10.7 index. The training, validation and testing data are represented by blue, green and red lines respectively.

[3] https://www.space-track.org/

Copyright © 2025 Advanced Maui Optical and Space Surveillance Technologies Conference (AMOS) – www.amostech.com

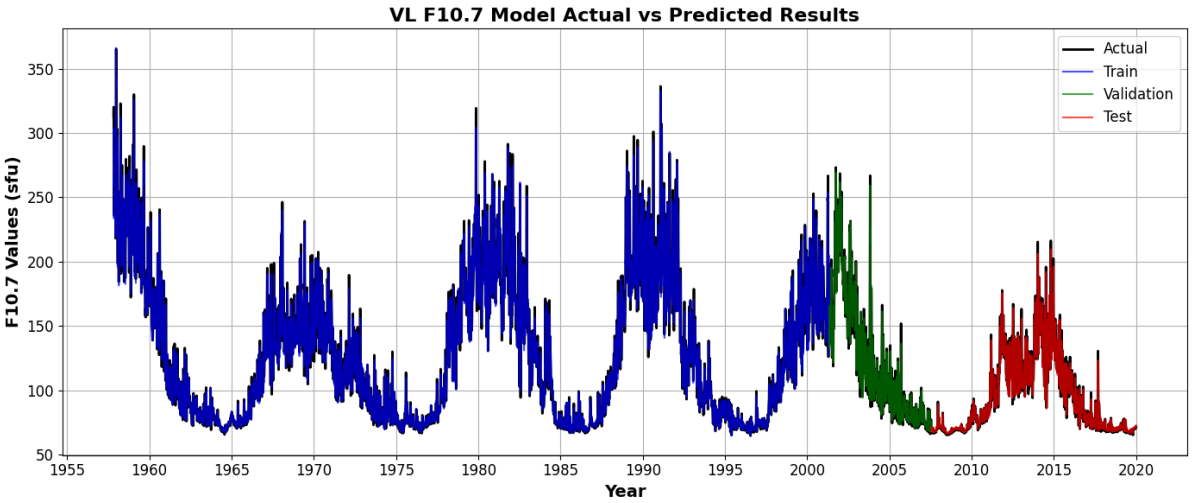

Figure 2: VL F10.7 model training (blue lines), validation (green lines) and testing (red) data sets for over 60 years.

The model error metrics, including RMSE and MAE for 3-day forecasts are reported in **Table 6** below.

Table 6: Error metrics for 3-day forecasts of the VL F10.7 model.

Metric	VMD-LSTM (VL) F10.7 Forecast
RMSE	2.17
MAE	1.53

Additionally, the performance of both models was evaluated on a held-out test set of low and high space weather activity, representing the most recent data, which was not used during training or validation. The primary metrics for comparison are the RMSE and MAE for a 3-day (72-hour) forecast horizon.

3.1.2 Quiet Case (July 1 – 3, 2025)

The VL models are used to forecast Kp and F10.7 values for a low geomagnetic activity period. The model vs truth RMSEs and MAEs are listed in **Table 7** below.

Table 7: Model performance metrics on 3-days test data for quiet case (July 1-3, 2025)

Metric	Kp Forecast		F10.7 Forecast	
	VL Kp	CT Kp	VL F10.7	CT F10.7
RMSE	8.96	18.64	8.25	13.66
MAE	7.62	15.33	7.86	13.36

VL models for both Kp and F10.7 are showing lower errors compared to CT forecasts for the quiet duration. We take a look at the comparison plots of Kp to understand the model behaviours.

As seen in **Figure 3**, for the quiet-time case the VL Kp model is estimating relatively stable, low Kp values. Whereas the CT Kp forecasts are unusually high, even predicting a minor (G1-level) storm that did not occur.

Copyright © 2025 Advanced Maui Optical and Space Surveillance Technologies Conference (AMOS) – www.amostech.com

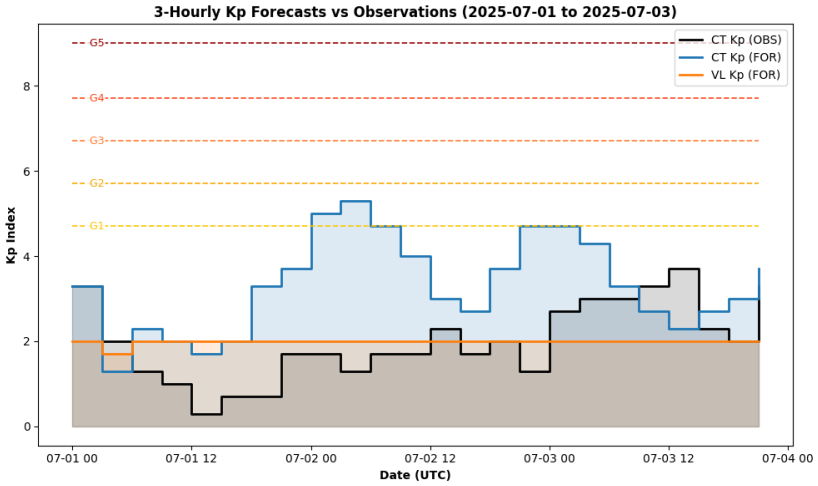

Figure 3: 3-day Kp forecasts vs observations for quiet case (July 1-3, 2025)

3.1.3 Storm Case (May 31 – June 2, 2025)

Both F10.7 and Kp VL models are further tested during the recent June 1 G4-level severe geomagnetic storm event. **Table 8** lists the forecast errors of VL and CT outputs.

Table 8: Model performance metrics on 3-days test data for storm case (May 31 – June 2, 2025)

Metric	Kp Forecast		F10.7 Forecast	
	VL Kp	CT Kp	VL F10.7	CT F10.7
RMSE	23.42	25.04	10.56	35.26
MAE	18.95	20.16	8.77	34.77

As we can see, both models perform better than corresponding CT forecasts. **Figure 4** shows that although CT Kp values increase during the storm initiation, it decreases fast for the main phase of the storm. Whereas the VL Kp values

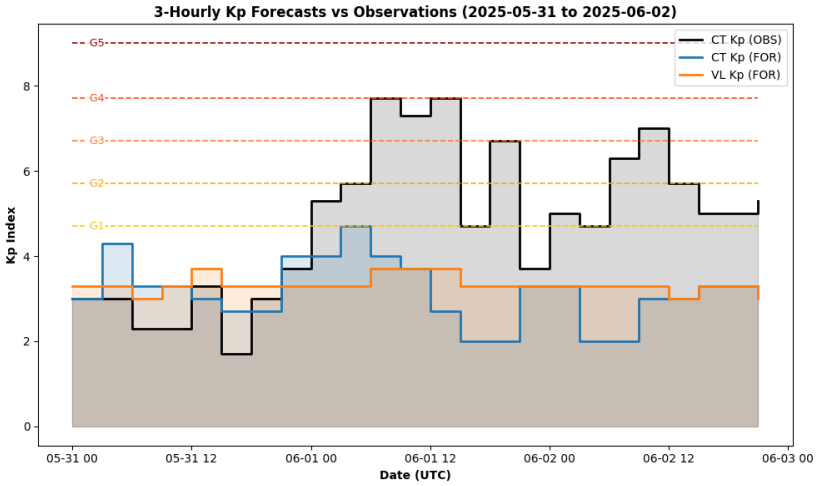

Figure 4: 3-day Kp forecasts vs observations for storm case (May 31 – June 2, 2025)

increase slightly during the storm and remain stable for the rest of its duration.

Copyright © 2025 Advanced Maui Optical and Space Surveillance Technologies Conference (AMOS) – www.amostech.com

3.2 Orbit Prediction Results

The synthetic satellites were propagated during both quiet and storm cases using the CT and VL space weather forecast outputs explained in the previous section. The model-generated orbits are compared with the reference true orbits (as explained in Section **2.3.2** by calculating the position difference in Earth Centered Inertial (ECI) frame. The models are evaluated using two error metrics – RMSE and position error over time. The position errors and RMSEs are evaluated against the reference orbits generated using observed space weather data. The error table and plots for all the test cases are as follows:

3.2.1 Quiet Case (July 1 - 3, 2025)

The position error plots for a 6U CubeSat at 450 km and 850 km altitudes can be seen in **Figure 5** below.

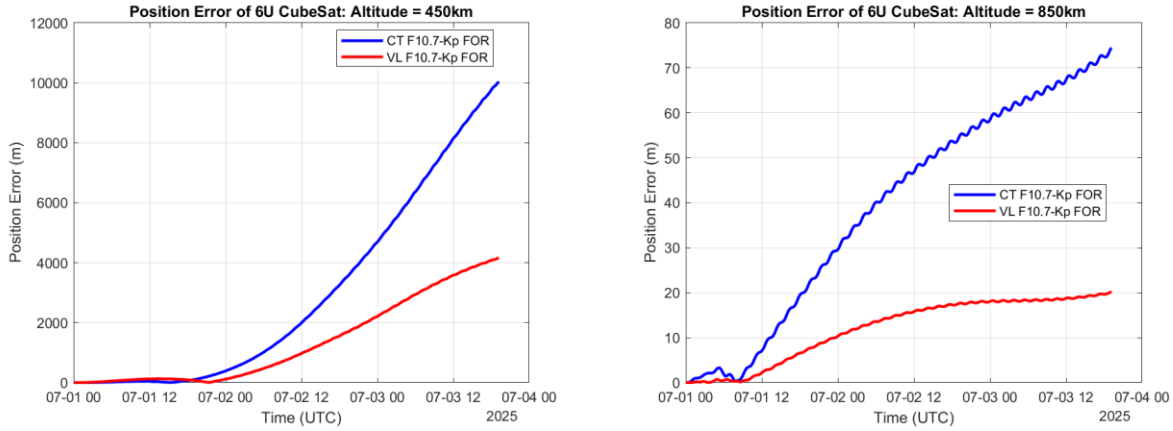

Figure 5: Position error of a 6U CubeSat at altitudes (a) 450 km (left) and (b) 850 km (right) during quiet-time propagation

For CubeSats at both low and high altitudes, orbit propagation using the VL space weather forecasts result in lower position errors compared to the CT forecasts under quiet geomagnetic conditions. As shown in **Table 9**, the position RMSE of the VL F10.7-Kp model is lower than that of the CT F10.7-Kp in most cases. At higher altitudes, the errors decrease significantly, consistent with the exponential decline of atmospheric density with altitude. Among individual drivers, the VL F10.7 model yields lower RMSE than the VL Kp model for most of the cases. When both VL forecasts are combined, further improvements in position accuracy are observed relative to the CT forecasts.

Table 9: Position RMSEs of CT and VL for all satellite configurations during the quiet case

Quiet Case: July 1 - 3, 2025					
CubeSat Size	**Altitude (km)**	**Position RMSE (m)**			
		CT F10.7-Kp	**VL F10.7-Kp**	**VL F10.7**	**VL Kp**
1U	450	906.2	263.3	152.3	472.6
	850	5.5	7.5	1.7	6.0
6U	450	4323.7	1923.2	697.1	1299.8
	850	45.9	13.9	5.7	18.9
12U	450	2107.5	956.6	436.9	537.8
	850	61.6	2.6	3.2	4.4
16U	450	2456.2	325.9	413.9	454.5
	850	74.4	4.5	3.7	1.0

Copyright © 2025 Advanced Maui Optical and Space Surveillance Technologies Conference (AMOS) – www.amostech.com

3.2.2 Storm Case (May 31 - June 2, 2025)

Figure 6 shows the relative position error plots for a 6U CubeSat at 450 km and 850 km altitudes.

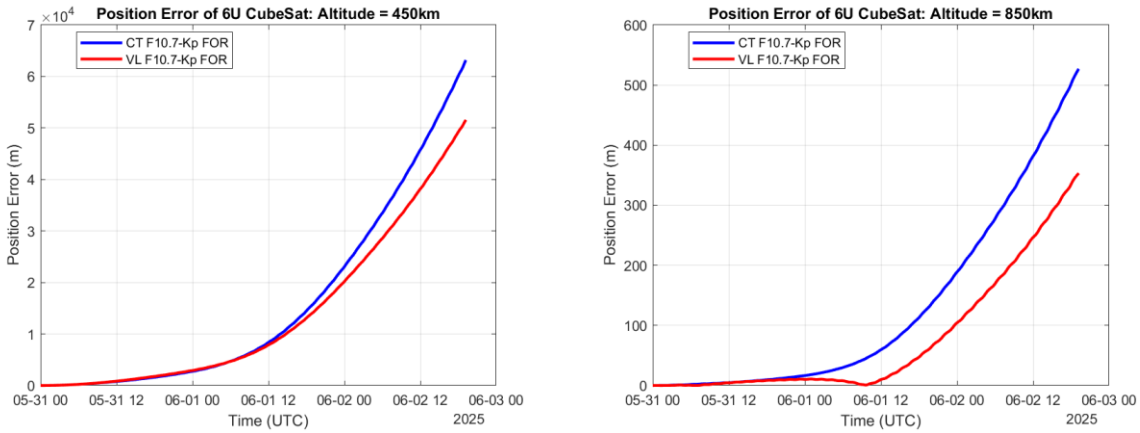

Figure 6: Position error of a 6U CubeSat at altitudes (a) 450 km (left) and (b) 850 km (right) during storm-time propagation

For propagation during the storm event, VL space weather forecasts produce trajectories with low prediction errors as compared to CT forecasts for CubeSats in both low and high altitudes.

Table 10 indicates that the relative position RMSE obtained with the VL F10.7-Kp model is generally lower than that of the CT F10.7-Kp model. In this case, the VL Kp model outperforms the VL F10.7 model, demonstrating the model's ability to capture storm-time variations. Overall, the combined forecasts from the VL model yield improved position accuracy compared to the CT forecasts.

Table 10: Position RMSEs of CT and VL for all satellite configurations during the storm case

Storm Case: May 31 - June 2, 2025					
CubeSat Size	**Altitude (km)**	**Relative Position RMSE (m)**			
		CT F10.7-Kp	**VL F10.7-Kp**	**VL F10.7**	**VL Kp**
1U	450	7067.1	6234.5	4710.4	2233.2
	850	77.8	22.2	55.5	21.0
6U	450	24054.2	20212.9	15727.3	5676.5
	850	199.3	126.0	123.2	71.4
12U	450	12939.7	10939.2	8584.4	3055.7
	850	117.3	111.8	74.5	42.8
16U	450	15611.3	13805.9	10016.5	4041.3
	850	190.0	171.1	142.5	113.2

3.3 Pc Estimation Results

Using the iterative collision probability estimation technique described in Section 2.4, Pc values were computed at TCA for each 3-hourly run. **Figure 7** presents the time series of Pc evolution obtained using the VL models at every 3-hour intervals until TCA. The results show that the VL Kp model maintains close agreement with the Pc values computed from reference space weather data up to 15 hours prior to TCA. The remaining VL models demonstrate consistency with the reference Pc values up to approximately 10 hours before TCA. It has been reported that many

Copyright © 2025 Advanced Maui Optical and Space Surveillance Technologies Conference (AMOS) – www.amostech.com

satellite operators wait till 12 – 24 hours from TCA [16] to take a call on maneuver decisions. Updating the object states with recent measurements constrains state uncertainties at that time. Following this approach, operators can potentially benefit from having at least 15 hours of conjunction notice to make a maneuver decision.

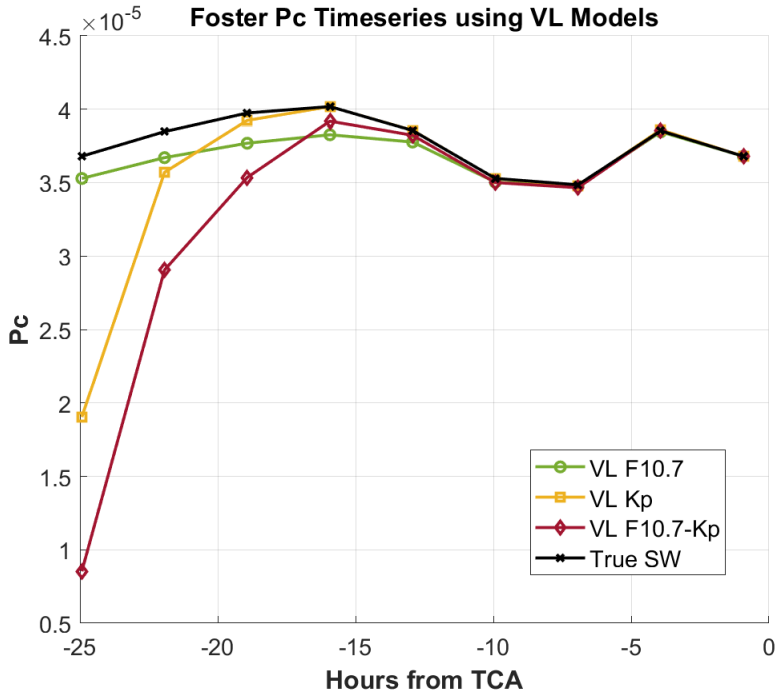

Figure 7: Pc timeseries of two objects calculated using VL models

The results demonstrate the efficiency of the VL forecasting models in realistic conjunction assessment and collision probability estimation scenarios.

4. CONCLUSION AND FUTURE WORK

This paper investigates the impact of space weather forecasting on LEO satellite operations and collision avoidance pipelines in this growing space era. We developed machine learning algorithms for F10.7 solar proxy and geomagnetic index Kp forecasting using VMD-LSTM architecture. These forecast models were further utilized to generate trajectories for synthetic LEO CubeSats of different sizes across varying altitudes. The obtained results were compared against reference orbits that use true space weather data. The results show that the VL space weather forecast-driven trajectories have lower errors than current operational forecasts available in CelesTrak. The iterative orbit propagation using VL model enables estimation of Pc values that are consistent with those obtained using true space weather inputs, but at earlier lead times, thereby improving the timeliness and reliability of conjunction assessment.

For future work, the Pc estimation method can be further modified to generate space weather forecasts for each iteration of state update and propagation run. We also plan to compare the performance of CelesTrak forecast-based Pc evolution against the VL model results. This will allow us to gauge the predictive accuracy of ML-based approaches as compared to traditional space weather forecasts in collision risk assessments. The VL model can be further optimized to generate faster and efficient forecasts.

With the rapid advancements in ML space (transformers, diffusion models, etc.), space weather forecasting can be significantly improved, leading to more reliable satellite operations in this congested and contested space environment.

5. ACKNOWLEDGEMENTS

This work was supported by Digantara Research and Technologies Pvt. Ltd. The authors thank the SSA team at Digantara for providing access to the proprietary orbit propagator, EPIC, and archived historical conjunction data

Copyright © 2025 Advanced Maui Optical and Space Surveillance Technologies Conference (AMOS) – www.amostech.com

from SOCRATES. The authors acknowledge the usage of CelesTrak, OMNIWeb, pymsis, etc. to obtain the required data and models utilized in this analysis.

REFERENCES

[1] W. E. Parker *et al.*, "Influences of Space Weather Forecasting Uncertainty on Satellite Conjunction Assessment," *Space Weather*, vol. 22, no. 7, Jul. 2024, doi: 10.1029/2023SW003818.

[2] W. E. Parker and R. Linares, "Satellite Drag Analysis During the May 2024 Gannon Geomagnetic Storm," *J Spacecr Rockets*, vol. 61, no. 5, pp. 1412–1416, 2024, doi: 10.2514/1.A36164.

[3] C. Bussy-Virat, A. Ridley, and J. Getchius, "Effects of Uncertainties in the Atmospheric Density on the Probability of Collision Between Space Objects," *Space Weather*, vol. 16, Aug. 2018, doi: 10.1029/2017SW001705.

[4] D. Gondelach, R. Linares, and P. M. Siew, "Atmospheric Density Uncertainty Quantification for Satellite Conjunction Assessment," *Journal of Guidance, Control, and Dynamics*, vol. 45, pp. 1–9, Aug. 2022, doi: 10.2514/1.G006481.

[5] Y. Y. Shprits, R. Vasile, and I. S. Zhelavskaya, "Nowcasting and Predicting the Kp Index Using Historical Values and Real-Time Observations," *Space Weather*, vol. 17, no. 8, pp. 1219–1229, Aug. 2019, doi: 10.1029/2018SW002141.

[6] L. Wang, H. Zhang, X. Zhang, G. Peng, Z. Li, and X. Xu, "Deep temporal convolutional networks for F_10.7 radiation flux short-term forecasting," *Ann Geophys*, vol. 42, no. 1, pp. 91–101, 2024, doi: 10.5194/angeo-42-91-2024.

[7] Y. Hao, J. Lu, G. Peng, M. Wang, J. Li, and G. Wei, "F10.7 Daily Forecast Using LSTM Combined With VMD Method," *Space Weather*, vol. 22, no. 1, p. e2023SW003552, 2024, doi: https://doi.org/10.1029/2023SW003552.

[8] K. Zhang *et al.*, "Forecasting Medium-Term F10.7 Using the Deep-Learning Informer Model," vol. 299, no. 4, p. 47, Apr. 2024, doi: 10.1007/s11207-024-02284-0.

[9] Sexton Ernest Scott, Nykyri Katariina, and Ma Xuanye, "Kp forecasting with a recurrent neural network," *J. Space Weather Space Clim.*, vol. 9, p. A19, 2019, doi: 10.1051/swsc/2019020.

[10] Y. Tan, Q. Hu, Z. Wang, and Q. Zhong, "Geomagnetic Index Kp Forecasting With LSTM," *Space Weather*, vol. 16, no. 4, pp. 406–416, 2018, doi: https://doi.org/10.1002/2017SW001764.

[11] G. Kervalishvili, I. Michaelis, M. Korte, J. Rauberg, and J. Matzka, "A Novel Model for Forecasting Geomagnetic Indices Using Machine Learning," *Geophys Res Lett*, vol. 52, no. 8, p. e2025GL114848, 2025, doi: https://doi.org/10.1029/2025GL114848.

[12] K. Dragomiretskiy and D. Zosso, "Variational Mode Decomposition," *IEEE Transactions on Signal Processing*, vol. 62, no. 3, pp. 531–544, 2014, doi: 10.1109/TSP.2013.2288675.

[13] F. A. Gers, J. Schmidhuber, and F. Cummins, "Learning to forget: continual prediction with LSTM," in *1999 Ninth International Conference on Artificial Neural Networks ICANN 99. (Conf. Publ. No. 470)*, 1999, pp. 850–855 vol.2. doi: 10.1049/cp:19991218.

[14] J. L. Foster and H. S. Estes, *A parametric analysis of orbital debris collision probability and maneuver rate for space vehicles*. NASA, National Aeronautics and Space Administration, Lyndon B. Johnson Space~…, 1992.

[15] T. S. Kelso and S. Alfano, "Satellite Orbital Conjunction Reports Assessing Threatening Encounters in Space (SOCRATES)," *Proceedings of SPIE - The International Society for Optical Engineering*, Aug. 2006, doi: 10.1117/12.665612.

[16] L. C. D. Moomey, R. Falcon, and A. Khan, "Trending and analysis of payload vs. All low earth conjunction data messages below 1000 km, from 2016 through 2021," *Journal of Space Safety Engineering*, vol. 10, no. 2, pp. 217–230, 2023, doi: https://doi.org/10.1016/j.jsse.2023.03.006.

Copyright © 2025 Advanced Maui Optical and Space Surveillance Technologies Conference (AMOS) – www.amostech.com